Deep Driving with Additional Guided Inputs for Crossings in Pedestrian Zones

Qazi Hamza Jan, Jan Markus Arnold Kleen and Karsten Berns
Robotic Research Lab, Department of Computer Science, Reinland Pfälzische-Technische Universität,
Erwin-Schrödinger-Straße 52, 67663 Kaiserslautern, Germany

Keywords: Autonomous Driving, Deep Driving, Pedestrian Zones, Simulation, Neural Networks, Directional Inputs.

Abstract: Deep Neural Networks are being used in different applications to solve complex tasks with high precision. One application, also the focus of this paper, is end-to-end driving. Generally, in an end-to-end approach, a neural network learns to directly feed values to actuators based on sensor inputs. This paper uses an End-to-end approach with images and additional direction inputs:*left, right and straight* for imposing a certain direction at unstructured and arbitrary intersections of pedestrian zones. Expecting high precision for predicted steering in pedestrian zones could be uncertain due to the atypical structures of intersections. Findings for increased accuracy are done using direction inputs with three variants of two approaches: Single and parallel model. Depth information was included to overcome shadow problems from RGB in simulation, but it resulted in worsening the drive, and hence removed in further experiments. The experiments are performed in simulation to verify the utility of the proposed approaches and narrow down the best models for actual hardware. From the experiments, it is seen that parallel model with front images have performed best. The model drove well along the paths and followed the given input direction from the user at the crossings. To maintain the length of this paper, only results for parallel structures are discussed.

1 INTRODUCTION

Automotive industries are working towards safer, reliable and human-like driving. Over the past few years, various aspects of autonomous driving are progressing (Parekh et al., 2022). Researchers benefit from Machine Learning (ML) algorithms for object detection (Tian et al., 2019; Erhan et al., 2014), semantic segmentation (Garcia-Garcia et al., 2017; Yu et al., 2018), vehicle control (Kuutti et al., 2020) etc. To take advantage of such encouraging results, this work uses an End-to-End deep neural network for driving autonomous vehicles in pedestrian zones. A pedestrian zone, in semantic perspective, offer a high variation in its architecture. It consists of unevenly connected paths. One such example with similar characteristics is shown in Figure 1. Autonomous vehicles in pedestrian zones are getting more attention (Jan et al., 2020b; Keen et al., 2021; Alvarez et al., 2019; Li et al., 2021).

This work deals with the challenges of driving an autonomous vehicle in uneven pathways and following a given direction at a high degree of varying cross sections. For initial validation of the technique proposed for this work, experiments are performed in a

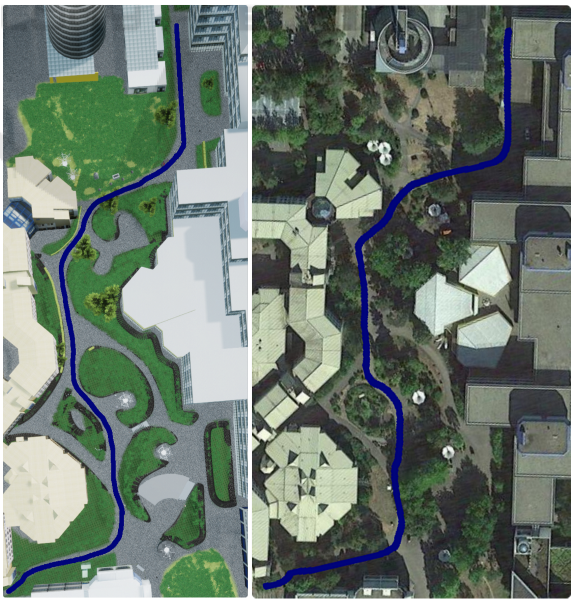

Figure 1: Top view of a small area of RPTU campus. The left image is a simulated model of the campus in the right image. The blue line shows the line sights the test drive of the model trained on the entire campus.

Jan, Q., Kleen, J. and Berns, K.
Deep Driving with Additional Guided Inputs for Crossings in Pedestrian Zones.
DOI: 10.5220/0011999600003479
In *Proceedings of the 9th International Conference on Vehicle Technology and Intelligent Transport Systems (VEHITS 2023)*, pages 402-409
ISBN: 978-989-758-652-1; ISSN: 2184-495X

simulation environment shown on the left of Figure 1, a replica of the real environment on the right. The environment is taken from our previous work in (Jan et al., 2020a; Jan et al., 2021). The gray texture in the simulation is the walking and driving zone connecting buildings within the campus.

End-to-end deep driving (Tampuu et al., 2020; Pomerleau, 1988; Muller et al., 2005; Bojarski et al., 2016; Codevilla et al., 2018), also known as behavior reflex, methodology processes the input sensory data directly and generates actuator values. Majority of researchers use RGB cameras as input (Kaur et al., 2021; Parekh et al., 2022; Toromanoff et al., 2018) and control the steering and velocity of the vehicle. Driving in an urban street environment has the simplicity of clear markings and lanes with fixed geometric crossings. On the contrary, pedestrian zones not only offer anfractuous pathways but also irregular crossways.

To solve the problem of selecting the designated path for the goal at intersections, authors have used route planners such as TomTom and OSM maps (Hecker et al., 2018). They claim that using a route planner gives better prediction of steering angle. For complex navigation systems, multiple approaches are used which carry its own syntax of giving direction to the destination. Such syntax can not always be integrated in the higher level map. To tackle such problem, this work implements generic directions: *left*, *right* and *straight* are applied for signaling at the intersections. For this work, the type of turning is ignored, for example, sharp turn, fork turn, etc. Since there are various shapes of crossing, it is not possible to assign them to a particular category. Hence, fixed generic commands were chosen based on driver intuition to the crossing angle.

The vehicle used for this work is a type of minibus, which is mounted with three cameras. The configuration is explained in Section 2. This study drew partial inspiration from (Codevilla et al., 2018). To realize the effect of different variables in the training process, multiple inputs are used: three cameras (RGB and depth images), speed, direction, steering values and throttle. Details are given in Section 2.

For this work, two types of approaches: single and parallel models are exploited with three variants based on number of cameras and the use of velocity input. These approaches are explained in Section 3.

Note. All the variants include direction inputs along with the combination of other inputs. Due to unavailability of such data with particular inputs, data gathering process is also part of this work discussed in the next section. Detailed experiments are given in section 4. From the aforementioned discussion, the novelty of this work can easily be articulated as following:

- Data collection
- Model creation
- Examining the effect of single and parallel models including the combination of all the input variants.
- Interpreting the effect of shadows
- Deciding for best approach

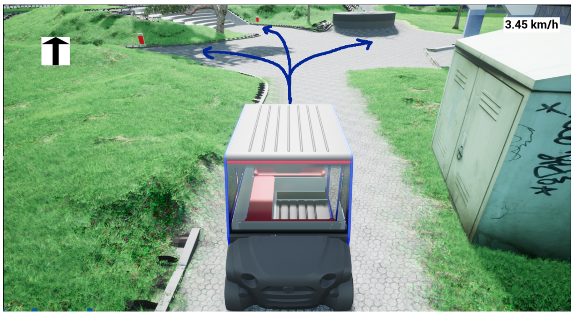

Figure 2: A virtual replica of vehicle and campus in simulation. The vehicle is a driver-less minibus used in the campus (Jan and Berns, 2021).

2 DATA COLLECTION

Unreal Engine[1] (UE), a game development tool, is used for training and testing models in this work. UE offers a realistic rendering which supports the use of visual sensors. The vehicle and RPTU campus were recreated in the simulation as shown in Figure 2. A comparison of the virtual and real world can be seen in Figure 1. The proposed work was conducted in simulation due to the following reasons:

- **Simplicity.** Since the neural network requires a huge amount of data to train the network, it is not

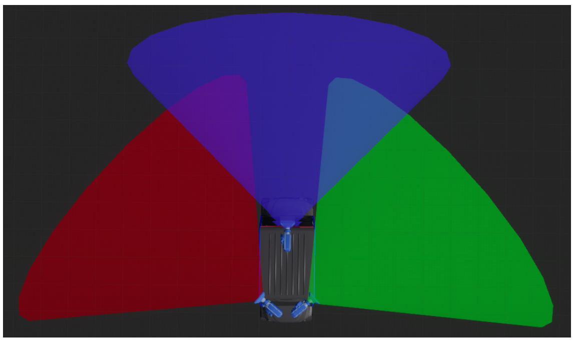

Figure 3: Camera configuration on the bus. It consists of front, rear-left and rear-right cameras. The configuration is similar to the on used for the actual robot (Jan et al., 2022).

[1]https://www.unrealengine.com/

laborious work, compared to real systems, to do such kind of initial testing in simulation.

- **Accessibility.** It was possible to collect data in locations where a real vehicle can not drive due to temporary restrictions or constructions.
- **Safety.** Most concerning aspects of driving in a pedestrian zone are the pedestrians. In view of the fact that vehicles and pedestrians have to share the same space, it becomes critical to have safe driving. In the real world, such concerns hinder testing.
- **Exploitation.** Simulation allows us to simulate every feature of the environment. Therefore the validation of reasoning becomes easy.

For data collection, the vehicle was driven by a human driver with an average speed of 6 *km/h* (restricted speed in pedestrian area). The vehicle was equipped with three cameras, configuration shown in Figure 3. Using three cameras amplifies the surrounding view relative to the front of the vehicle. To cater the shadow problem, additional depth images were taken into account. Hence, the system is able to drive in varying light conditions.

Data was collected every 0.5 seconds. It consisted of the following information:

- RGB images from all the three cameras shown in Figure 3
- Depth image from the front camera
- Current speed of the vehicle
- Current throttle as a floating value from -1 to 1
- Three direction commands as integer: 0-straight, 1-left and 2-right
- Timestamp
- Addition comments

During the training of the model, since a human was driving the vehicle with a certain direction and average speed; throttle, steering and directions were recorded directly from the user. To keep track of countless situations and conditions such as presence of pedestrians, presence of shadow, type of configuration, variant kind and so on, were encoded in additional comments. 76 driving sequences were performed with more than 30000 frames recorded in total. Driving itself was based solely on the operator. The operator steered the vehicle using a joystick. Speed of the vehicle was usually kept constant to a human walking speed. In order to give the direction, the operator was told to press the given key number assigned to the respective direction once the intersection was fully visible. By default, straight-direction was enabled regardless of size or curve of a standard path. One particular scene, with possible turning, is overlaid in Figure 2. The blue arrow shows the driver's intuition of a possible driving path at the cross section.

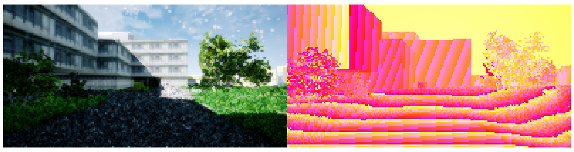

Figure 4: The figure assimilates RGB data to the corresponding depth data. Undoubtedly, the shadow is indiscernible in depth image.

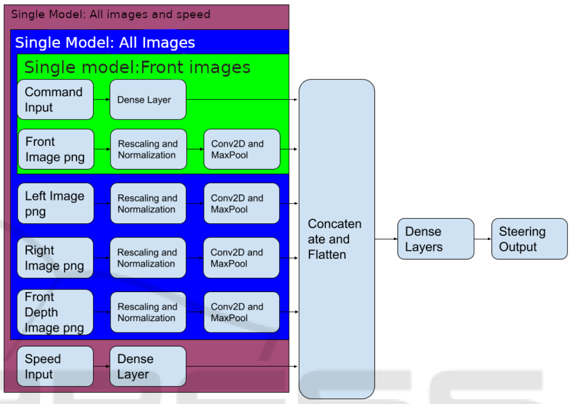

(a) Network structure for all images and speed.

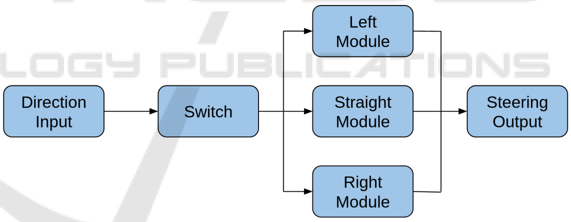

(b) Single network structure from above image used separately for different directions.

Figure 5: (a) *Single Model:* Single network structure for input with all images and speed. (b) *Parallel model:* The left, right and straight modules are equivalent to the single structure as in the top image, except for the command input which is used to switch between the three models.

3 APPROACH

Unlike single images given as input for classification and detections (Hoiem et al., 2005; Zhu et al., 2014), the model implemented for this work uses multiple inputs with varied configuration. One of the objective was to explore different combinations of inputs and model type for better results. The division of applied approaches is given in flow chart of Figure 6. Firstly, the approach was bifurcated into a single and paral-

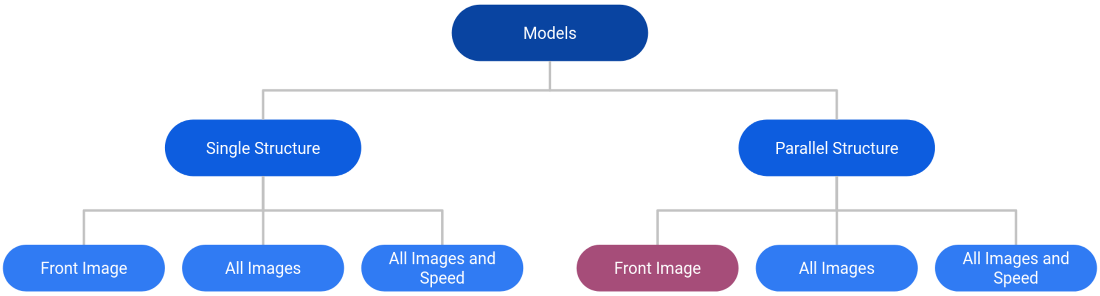

Figure 6: Block diagram for two variations of model: single and parallel models including the direction inputs with three variants of input: front camera, all cameras, and all camera with velocity.

lel model. The Basis of such bifurcation was a training model with direction data. Single structure, as the name suggests, has one model trained with all the direction inputs. For parallel model, sub-models consisting of each single structure were tabulated specific to one direction input. One model was activated based on direction input by a switching technique. The design of both models can be seen in Figure 5. The convolution neural networks are modified to the given inputs. After concatenation and flattening, dense layers are used for output prediction of steering. For clarity, the variants are segregated in to different color segments shown in Figure 5a. The green segment shows input for the first variant, the blue shows the inputs for the second input and maroon color shows the inputs for all inputs including green and blue segments.

The last layer of Figure 6 gives the type of inputs for testing precision. The models were tested first with only the front camera, then with all the three cameras, and finally using additional speed input with all cameras. Using all cameras confirms the effect of a wide view on driving. Speed was added to check the impact on steering values.

4 EXPERIMENTS

The experiments were performed in the same campus environment by giving different directions at crossings and adding other props for reasoning of unusual behavior. This section explains the prediction error for all the models and based on the best performance, the respective model is chosen for further evaluation.

4.1 Prediction Errors

As a first step in evaluating the network, model predictions were compared to the ground truth that was recorded when gathering training data. For each model, a subset of data points are randomly selected which is compared to human driving (the training set). Mean Square Error (MSE) can be calculated with the given data which is demonstrated in Table 1.

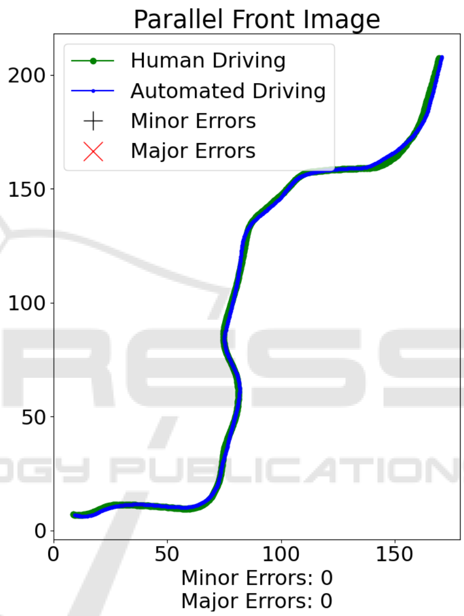

Figure 7: Comparison plot of Trajectory for testing and ground truth.

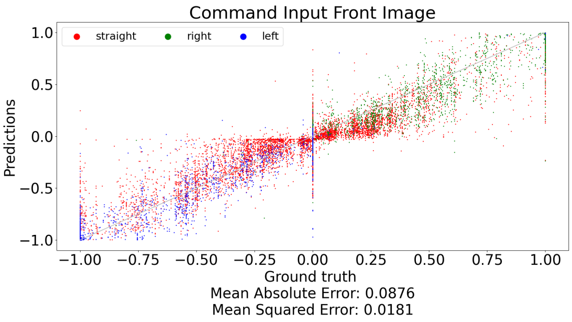

Figure 8: Relationship between the steering predictions of *Single Front Images* model and steering of human driver.

Further investigating from Table 1, single model with all variants shows high variances in performance between different directions, the spread can be seen

Table 1: Mean Squared Error of predictions and ground-truth.

Model	Used Camera	Speed Input	All	Straight	Left	Right
Single	Front	No	0.0181	0.0169	0.0214	0.0229
	All	No	0.0214	0.0183	0.0185	0.0418
	All	Yes	0.0290	0.0247	0.0497	0.0385
Parallel	Front	No	0.0219	0.0233	0.0237	0.0206
	All	No	0.0174	0.0168	0.0204	0.0201
	All	Yes	0.0225	0.0230	0.0213	0.0202

Table 2.

Model	Minor Errors	Major Errors
Single:Front Image	1	5
Single:All Images	5	4
Single:All images, speed	4	7
Parallel:Front Image	0	0
Parallel:All Images	3	0
Parallel:All images, Speed	2	1

in Figure 8. One reasoning for this could be the unequal distribution of the training data. Unequal distribution of data in terms of direction is coherent to the fact that encountering crossings is seldom than driving paths between the crossings in pedestrian zones. Hence, this results in over-fitting of the model for this direction. On the other hand, parallel models in which each model is trained for a particular direction, do not suffer drastically from this problem. The unequal distribution does not affect the trained model because every model is directed to one direction.

The inclusion of speed data in the model reduces the accuracy of the overall model for both structures. Incorporating the left and right cameras along with the front camera pertain to ambiguity in comprehending the results. Although, using additional cameras increases the range of view, it also amounts for more unnecessary information such as the patches enclosing the pedestrian walk. Despite the sub-models of the parallel structure being trained individually on less data compared to a single structure, it performs similarly if not better. This is established in the next subsection.

4.2 Real-Time Testing

Following the insights of all the models by comparison of model predictions with ground truth, it is not sufficient to claim the credibility of the model in terms of standard driving. Further performance evaluation is done by letting the model drive the vehicle in a simulated environment with the user directing at intersections by giving one of the three direction inputs.

4.2.1 All-Model Testing

The tests were done on different routes of the campus, but on the account of comparison, a specific path was chosen marked with blue in the Figure 1. A trajectory comparison for Parallel model with front image is given in Figure 7. For quantifying the results, the term minor and major error was established. Vehicle going off-path during driving was considered a minor error, whereas wrong turns or colliding into obstacles was defined as a major error. The comparison can be seen in Table 2.

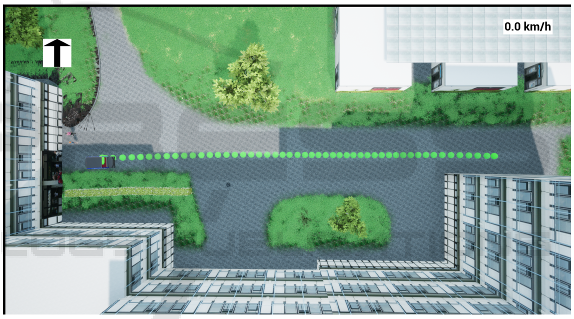

(a) Green dotted line shows the path driven by user during the training process.

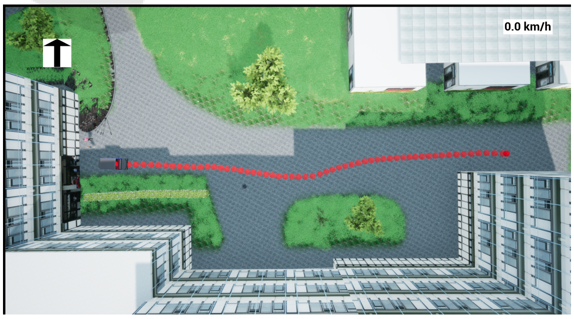

(b) Red dotted line shows the path of driving during the test phase.

Figure 9: The images show the top view of driving path by human (top) and model (bottom). The curve in the bottom image shows the effect of shadow on the network.

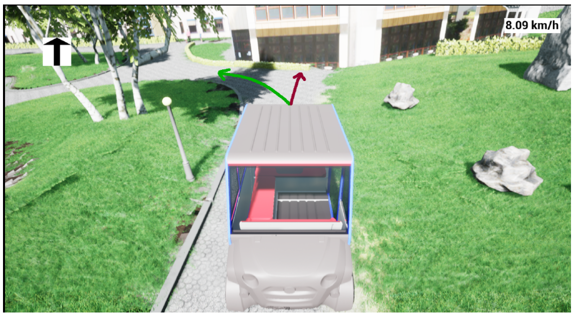

Figure 10: Effect of shadow on driving. The green arrow shows the consistent path driven by the user. Red arrow indicates the path driven by the network.

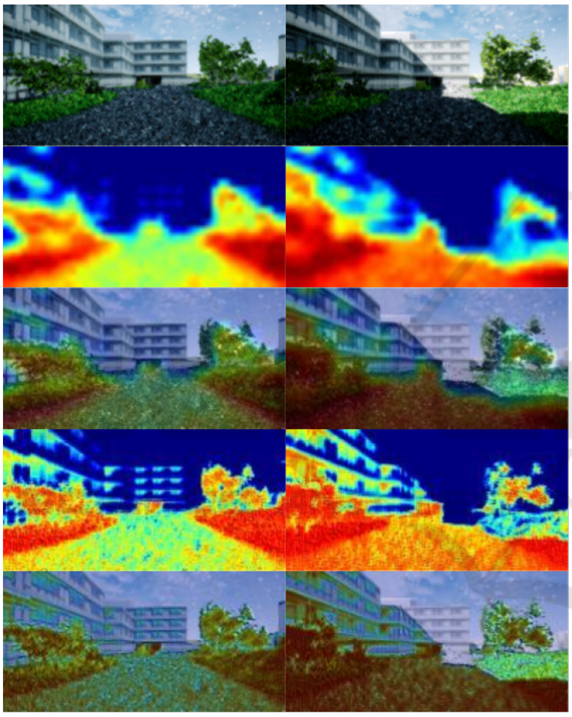

Figure 11: The attention maps from the model for two similar scenarios taken from two convolution layers. One consists of shadow and one without shadow.

4.2.2 Shadows

Shadows were the major problem identified during the phase of testing. The network was unable to detect the true path in the presence of a shadow. One particular example is shown from the top view in Figure 9. The top image shows the vehicle driven by a human. Shadows were always ignored when driven by a human throughout the campus. Strikingly, the model understood the change in contrast of shadow and non-shadow region as the boundary of the path. This is implied by the slight curve of the red dotted line in Figure 9b. For justification of this interpretation, another example with similar context is presented in Figure 10. Green arrow shows the user driven pathways, and red arrow is wrongly driven by the network. To visualize the effect of shadows, attention map from network layer was overlaid over RGB image seen in Figure 11. The second row from above in Figure 11 shows the attention map from a shallow layer of the network, while the fourth row shows the attention map from a deep layer of the network. The color gradient shows that the system perceives shadows as boundary regions and does not consider as drivable region. Also, the red regions enables the vehicle to move in a straight path.

4.2.3 Depth Images

Researchers have used depth images to tackle shadows in RGB images (Krywolt, 1993; Bi et al., 2022; Xiao et al., 2014). Depth images are invariant to shadows existing in color images. A clear example is illustrated in Figure 4. The comparison shows that the depth clearly ignores the disparity caused by shadows. Initially, it was proposed to use depth images as additional input due to aforesaid reasons. Throughout the tests, the driving was recurrently skewed from the given pathway. Observing the depth images, it is not easy to differentiate between pathways and surrounding areas. In other words, there exist no clear boundaries. Environments, such as used for this work, have plain grass surrounding the paths. From a depth perspective, it is difficult to differentiate between such regions. Figure 12 extracts the silhouettes of ground from depth image of Figure 4 to see this relation. For this scene, the silhouettes slightly rise at the corners. As a result, the depth images were removed from further testing.

Figure 12: Silhouette for ground region from depth image shown in Figure 4.

4.2.4 Blockage Effect

In a specific region, there was one instance where the system experienced difficulty in identifying the correct path and accurately interpreting commands, as depicted in the figure 13. Evidently, the system mistakenly perceived the large paved area ahead of the vehicle as a dead end, akin to a parking space, and consequently interpreted it as the designated route to drive on when instructed to proceed straight. The environment in question comprises authentic dead ends that the system is trained to navigate through. Notably, the straight command directs the system to follow the path in a manner consistent with human interpretation of following the correct curve. However, it is important to note that the same command can be issued by an operator intending to park the vehicle in this space, which underscores the potential ambiguity of the commands. Thus, there is likely a need for additional commands to enhance the system's functionality. The green arrow shows the drivable path for this region, red arrow shows the predicted path.

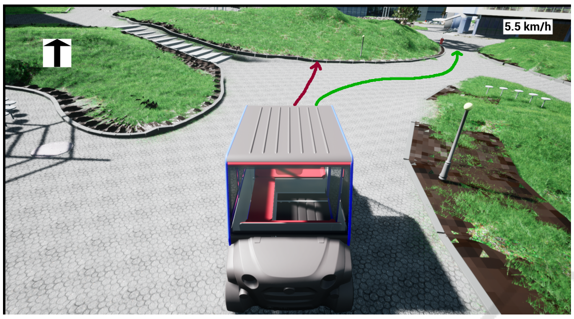

Figure 13: The system can not identify the right curve as the correct choice and drives in a straight line as shown by Red arrow, colliding with the grass hill if not stopped. Changing the command to *"right"* causes the vehicle to follow the right curve illustrated by blue arrow, but this should not be needed as the *straight* command means following the path.

To explore this issue in greater depth, an obstruction in the form of a wall was introduced in the front area. Despite the absence of such a blockage in the training phase, the system successfully identified the correct path and operated in accordance with it. As depicted in Figure 14, the driving path is indicated by the blue arrow. One possible explanation for this outcome is that the system regarded the stairs located on the opposite side of the drivable area as a viable path and thus took a middle course. The introduction of the obstruction enabled the system to clearly discern a single path to follow.

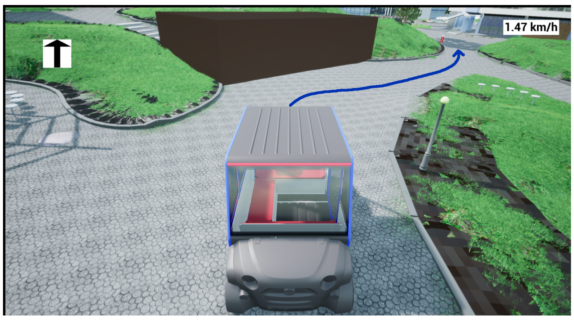

Figure 14: The same situation as in figure 13, but the front and right stair region is blocked off. The system is now able to identify the right curve (blue arrow) as the correct choice with *straight* input.

5 CONCLUSIONS

This paper explores the possibility of using directions as input to a neural network for crossings in pedestrian zones. The network was able to follow the commands correctly and navigate throughout the path. Based on the number of cameras, speed input and configuration possibility, different models were developed and evaluated against each other. From the findings, it is suggested that using a parallel approach (having direction specific input sub-model) performs better than a single model trained on all the given direction inputs. While the results are encouraging, the performance lag in some conditions such as lighting conditions. Depth image, proposed solution for shadow problem in simulation, did not assist in overcoming lighting problem. In fact, depth added more uncertainty. These shortcomings could be resolved by further training the system in various environments and situations, especially situations where the vehicle is required to recover from a suboptimal position.

REFERENCES

Alvarez, W. M., De Miguel, M. A., García, F., and Olaverri-Monreal, C. (2019). Response of vulnerable road users to visual information from autonomous vehicles in shared spaces. In *2019 IEEE Intelligent Transportation Systems Conference (ITSC)*, pages 3714–3719. IEEE.

Bi, X., Yang, S., and Tong, P. (2022). Moving object detection based on fusion of depth information and rgb features. *Sensors*, 22(13):4702.

Bojarski, M., Del Testa, D., Dworakowski, D., Firner, B., Flepp, B., Goyal, P., Jackel, L. D., Monfort, M., Muller, U., Zhang, J., et al. (2016). End to end learning for self-driving cars. *arXiv preprint arXiv:1604.07316*.

Codevilla, F., Müller, M., López, A., Koltun, V., and Dosovitskiy, A. (2018). End-to-end driving via conditional imitation learning. In *2018 IEEE international conference on robotics and automation (ICRA)*, pages 4693–4700. IEEE.

Erhan, D., Szegedy, C., Toshev, A., and Anguelov, D. (2014). Scalable object detection using deep neural networks. In *Proceedings of the IEEE conference on computer vision and pattern recognition*, pages 2147–2154.

Garcia-Garcia, A., Orts-Escolano, S., Oprea, S., Villena-Martinez, V., and Garcia-Rodriguez, J. (2017). A review on deep learning techniques applied to semantic segmentation. *arXiv preprint arXiv:1704.06857*.

Hecker, S., Dai, D., and Van Gool, L. (2018). End-to-end learning of driving models with surround-view cameras and route planners. In *Proceedings of the european conference on computer vision (eccv)*, pages 435–453.

Hoiem, D., Efros, A. A., and Hebert, M. (2005). Geometric context from a single image. In *Tenth IEEE International Conference on Computer Vision (ICCV'05) Volume 1*, volume 1, pages 654–661. IEEE.

Jan, Q. H. and Berns, K. (2021). Safety-configuration of autonomous bus in pedestrian zone. In *VEHITS*, pages 698–705.

Jan, Q. H., Kleen, J. M. A., and Berns, K. (2020a). Self-aware pedestrians modeling for testing autonomous vehicles in simulation. In *VEHITS*, pages 577–584.

Jan, Q. H., Kleen, J. M. A., and Berns, K. (2021). Simulated pedestrian modelling for reliable testing of autonomous vehicle in pedestrian zones. In *Smart Cities, Green Technologies, and Intelligent Transport Systems: 9th International Conference, SMARTGREENS 2020, and 6th International Conference, VEHITS 2020, Prague, Czech Republic, May 2-4, 2020, Revised Selected Papers 9*, pages 290–307. Springer.

Jan, Q. H., Klein, S., and Berns, K. (2020b). Safe and efficient navigation of an autonomous shuttle in a pedestrian zone. In *Advances in Service and Industrial Robotics: Proceedings of the 28th International Conference on Robotics in Alpe-Adria-Danube Region (RAAD 2019) 28*, pages 267–274. Springer.

Jan, Q. H., Wolf, P., Berns, K., Reich, J., and Wellstein, M. (2022). Integration of human skeleton posture models into reaction for realizing dynamic risk management.

Kaur, P., Taghavi, S., Tian, Z., and Shi, W. (2021). A survey on simulators for testing self-driving cars. In *2021 Fourth International Conference on Connected and Autonomous Driving (MetroCAD)*, pages 62–70. IEEE.

Keen, H. E., Jan, Q. H., and Berns, K. (2021). Drive on pedestrian walk. tuk campus dataset. In *2021 IEEE/RSJ International Conference on Intelligent Robots and Systems (IROS)*, pages 3822–3828. IEEE.

Krywolt, R. W. (1993). *Post-Processed Shadow Determination for Composition of Depth Images*. PhD thesis, University of British Columbia.

Kuutti, S., Bowden, R., Jin, Y., Barber, P., and Fallah, S. (2020). A survey of deep learning applications to autonomous vehicle control. *IEEE Transactions on Intelligent Transportation Systems*, 22(2):712–733.

Li, Y., Cheng, H., Zeng, Z., Liu, H., and Sester, M. (2021). Autonomous vehicles drive into shared spaces: ehmi design concept focusing on vulnerable road users. In *2021 IEEE International Intelligent Transportation Systems Conference (ITSC)*, pages 1729–1736. IEEE.

Muller, U., Ben, J., Cosatto, E., Flepp, B., and Cun, Y. (2005). Off-road obstacle avoidance through end-to-end learning. *Advances in neural information processing systems*, 18.

Parekh, D., Poddar, N., Rajpurkar, A., Chahal, M., Kumar, N., Joshi, G. P., and Cho, W. (2022). A review on autonomous vehicles: Progress, methods and challenges. *Electronics*, 11(14):2162.

Pomerleau, D. A. (1988). Alvinn: An autonomous land vehicle in a neural network. *Advances in neural information processing systems*, 1.

Tampuu, A., Matiisen, T., Semikin, M., Fishman, D., and Muhammad, N. (2020). A survey of end-to-end driving: Architectures and training methods. *IEEE Transactions on Neural Networks and Learning Systems*.

Tian, Y., Yang, G., Wang, Z., Wang, H., Li, E., and Liang, Z. (2019). Apple detection during different growth stages in orchards using the improved yolo-v3 model. *Computers and electronics in agriculture*, 157:417–426.

Toromanoff, M., Wirbel, E., Wilhelm, F., Vejarano, C., Perrotton, X., and Moutarde, F. (2018). End to end vehicle lateral control using a single fisheye camera. In *2018 IEEE/RSJ International Conference on Intelligent Robots and Systems (IROS)*, pages 3613–3619. IEEE.

Xiao, Y., Tsougenis, E., and Tang, C.-K. (2014). Shadow removal from single rgb-d images. In *Proceedings of the IEEE Conference on Computer Vision and Pattern Recognition*, pages 3011–3018.

Yu, C., Wang, J., Peng, C., Gao, C., Yu, G., and Sang, N. (2018). Bisenet: Bilateral segmentation network for real-time semantic segmentation. In *Proceedings of the European conference on computer vision (ECCV)*, pages 325–341.

Zhu, M., Derpanis, K. G., Yang, Y., Brahmbhatt, S., Zhang, M., Phillips, C., Lecce, M., and Daniilidis, K. (2014). Single image 3d object detection and pose estimation for grasping. In *2014 IEEE International Conference on Robotics and Automation (ICRA)*, pages 3936–3943. IEEE.